Article

Atmospheric CO_2 Two Box Model Accurately Tracks 14C and 13C without Requiring the "Revelle Isotopic Exception"

S E Taylor

Director, Geomatix Ltd, UK
* Correspondence: set@geomatix.net

Abstract

Although nett CO_2 flows can be estimated with reasonable accuracy, the contributing gross fluxes between the atmosphere and the earth's surface are poorly understood. This paper presents a means by which the global outflow and inflow of CO_2 between atmosphere and "mixing reservoirs" can be calculated, using the radiocarbon isotopes $^{14}CO_2$ and $^{13}CO_2$ as a tracer. It has been asserted that isotopic CO_2 cannot be directly used as a tracer in flow studies because $\Delta^{14}C$ is not subject to the Revelle factor; evidence is provided showing that this view is mistaken. The model contains 7 key parameters which are used to provide outputs of $\Delta^{14}C$ and $\delta^{13}C$ as a function of time. By optimising the fit of these two outputs with historical records spanning 200 years or more, including during the bomb pulse, the key parameters are determined. The quality of fit of $\Delta^{14}C$ and $\delta^{13}C$ is excellent and the internal parameters optimise at reasonable values. The global flux to and from the effective mixing reservoir, whose size is six times that of the atmosphere, is currently 58 GTC/yr in 2020, not including annually cycled carbon.

Keywords: CO_2 residence-time; CO_2 lifetime; anthropogenic emissions; global warming

Environmental Significance

An accurate estimate of the flux between the atmospheric and sequestered CO_2 is important as it is key to our understanding of the carbon-cycle, yet estimates of these fluxes have large uncertainties. This paper describes a method of calculating such atmospheric CO_2 flux by using the historical variations of $^{14}CO_2$ and $^{13}CO_2$ for calibration, challenging the view that such studies cannot be carried out because of a supposed anomalous isotopic effect. It also provides a new estimate of the fossil fuel airborne fraction and the accumulation of carbon inventory.

Introduction

The global CO_2 flux between the atmosphere and the earth's surface are poorly understood and difficult to calculate with considerable uncertainties in their estimation. Fig 6.1 of IPCC WG1 AR5 (Ciais 2013) states "Individual gross fluxes and their changes since the beginning of the Industrial Era have typical uncertainties of more than 20%." The existence of a sizeable CO_2 atmospheric gross inflow and outflow is frequently overlooked, partially because of the emphasis on Nett CO_2 flow and quasi-equilibrium models based upon a pre-industrial equilibrium. Yet if all atmospheric sources of CO_2 were switched off, few would deny that the atmospheric CO_2 mixing ratio would significantly decline, demonstrating that there must be a considerable sink flux. Nett variations in the source or sink flux are manifested by changes in the atmospheric level itself as it depletes or fills. Such variations are known to have occurred during the deglaciation between 16ka and 12ka, when changes in global temperature accompanied century-scale variations in

 doi:10.20944/preprints202212.0413.v1

CO_2 and $\delta^{13}C$ (Bauska et al. 2014, **Bengtson et al 2020, Marcott et al., 2014)**. Therefore changes in natural CO_2 flux should not be disregarded when accounting for atmospheric CO_2 fluctuations, especially when accompanied by a significant global temperature change, such as is recently becoming apparent. Throughout this document the phrases "atmospheric mixing ratio" and "atmospheric CO_2 level" are used interchangeably, while the term CO2ff refers to the anthropogenic fossil fuel CO_2 emissions. The calculations are provided in the form of a working Excel Spreadsheet. Since the analysis relies upon the atmospheric variations of $^{14}CO_2$ and $^{13}CO_2$ over the past 200 years, a brief historical perspective of atmopheric radiocarbon is now provided.

Radiocarbon Summary

The most abundant isotope of atmospheric carbon is the stable form ^{12}C, with around 1 part in 10^{12} being the radioactive isotope ^{14}C (ref) while around 1 percent is the non-radioactive isotope ^{13}C. Samples of wood, charcoal etc, provide an historical record of the atmospheric concentration of ^{14}C and ^{13}C, as carbon becomes embedded in the sample (Stenström 2011). However ^{14}C and ^{13}C exhibit very different properties; ^{14}C undergoes radioactive decay with a half-life of 5700 +/-30 years (Kutschera, W., 2013), while ^{13}C is radioactively stable. The ratiometric symbol for ^{14}C activity is $\Delta^{14}C$, which incorporates the necessary corrections for decay and fractionation so that comparison can be made across different ages. Fossil fuels, being hundreds of millions of years old, contain virtually no ^{14}C as it has already radioactively decayed. The combustion of fossil fuels therefore releases virtually no $^{14}CO_2$ into the atmosphere, thus diluting the ^{14}C atmospheric concentration; a process known as the "Suess Effect" (Suess 1955). By contrast with ^{14}C, the content of ^{13}C in fossil fuels is just a few percent below background levels of ^{13}C. This reduction is not due to radioactive decay but is caused by fractionation, arising because ^{13}C atoms are slightly larger and heavier than ^{12}C, and their corresponding reaction rates are slightly slower. During the conversion of atmospheric CO_2 to carbon within the sample, fractionation reduces the relative presence of ^{13}C (Stuiver & Quay 1981). Therefore, when fossil-fuels combustion adds CO_2 molecules to the atmosphere, the ^{13}C concentration falls, in a similar but much less pronounced way than that for ^{14}C. Before 1900 the $^{13}C/C$ ratio (written as $\delta^{13}C$) remained remarkably constant over the previous 10,000 years, maintaining its value to within +/- 0.1‰ (Bengston 2020). However, since 1900 its value has fallen sharply; by approximately 2‰. The $^{14}C/C$ ratio (written as $\Delta^{14}C$) was less stable, falling on average by around 2‰ per century over the past 10,000 years, occasionally falling by 8‰ in one century (IntCal20). However, its fall between 1900 and 1950 is much steeper, being 25‰ in only 50 years. Thus $\delta^{13}C$ and $\Delta^{14}C$ both show exceptional falls since 1900. For $^{14}CO_2$ since 1950 the picture is more complex, because of the creation of $^{14}CO_2$ by atomic weapons atmospheric tests. The decay of this "bomb pulse" (Figure 3) was initially exponential, perhaps indicating an ^{14}C absorption rate which was proportional to its concentration. However by 2020, although the atmospheric ^{14}C level is around zero, it is still falling significantly below zero, rather than levelling off to its pre-bomb value. Stuiver & Quay (1981) had measured ^{14}C in archived tree-ring samples confirming the pre-bomb "Suess Effect", but finding it was only 32% of the expected value, a margin they called the *"$^{14}CO_2/CO_2$ attenuation factor"* because *"part of the radiocarbon deficit is stored in the oceans and biosphere"*. Similarly, calculations of the Suess dilution of $^{13}CO2$ show that it too should be falling more steeply (see Appendix D). Levin (2009) has discussed the dilution discrepancy of $\Delta^{14}C$ and calculated a theoretical reduction rate due to CO2ff dilution alone as 12-14‰ per year which she suggested *"is partially compensated by $^{14}CO_2$ release from the biosphere, industrial $^{14}CO_2$ emissions and natural ^{14}C production."* The reader may be interested to note that while $\Delta^{14}C$ continues to fall, the absolute atmospheric content of ^{14}C has recently begun to increase (Svetlik 2010), reflecting the general atmospheric increase in CO_2.

Isotopic Ratiometric Exception

Preprints (www.preprints.org) | NOT PEER-REVIEWED | Posted: 22 December 2022 doi:10.20944/preprints202212.0413.v1

Regarding absorption of atmospheric CO_2 across the seawater surface boundary, it is widely known and accepted that the Revelle factor reduces the effective size of the surface-ocean reservoir due to chemical buffering. Boundary isotopic equilibrium is reached when the ratio of the two isotopic partial pressures match the inverse ratio of the fractionation factors, in and out (Appendix Eq. A7). Although the fractionation factor for photosynthesis is approximately 0.98, the seawater fractionation factors are even closer to unity, so close as to be irrelevant (Bolin and Eriksson 1959). Irrespective of this, it has been asserted that analysis of the decay of the "^{14}C bomb pulse" cannot be used to calculate atmospheric CO_2 flux because *"bomb radiocarbon and anthropogenic CO_2 do not behave identically.....the equilibration time is about ten times longer for ^{14}C than it is for anthropogenic CO_2"* (Joos 1994) and more recently *"The Revelle factor does not apply to isotopic equilibration because a $^{12}CO_2$ molecule is replaced by a $^{13}CO_2$ or vice versa. As a result, an isotopic anomaly disappears from the atmosphere more quickly than a total CO_2 anomaly." Tans 2022.* The assertion of the existence of such a large difference in the behaviour of an isotope compared to it non-radioactive form is unusual. It appears to originate from a mathematical derivation published by Tans 1993 eq. 16. The assertions have been widely repeated. (Harvey 2000, CiaisWG1 AR5 2013, Archer 2009). The author contends the notion arose because of an error and an omission in Tans' calculation, see Appendix A, which gave rise to a misinterpretation. In 1959 Bolin and Eriksson published CO_2 flux calculations where they derived both the Revelle factor and Suess effect, considering isotopic flow at a seawater-atmosphere boundary. They did not make the same claim regarding unfettered isotopic ratiometric diffusion. Further, regarding fractionation they stated "*The deviation of μ from unity will be completely irrelevant in the following discussion. We shall ... thus neglect fractionation.*" This approach was adopted in the model below. Fractionation rates have been set to unity, and the mistaken isotopic Revelle exception is not included.

CO_2 Finite Reserve Model

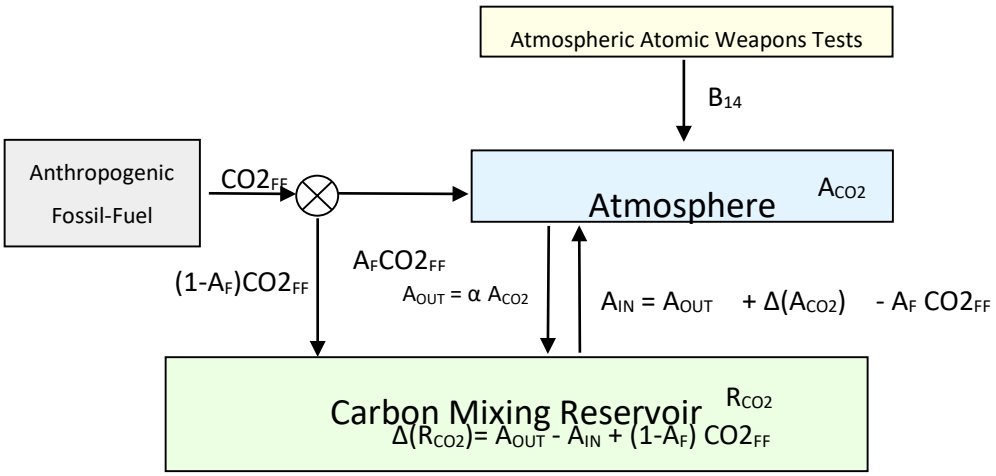

Figure 1: CO_2 Finite Reservoir Two Box Model

The CO_2 Finite Reserve Model (CFR) is a two box model describing CO_2 fluxes between an idealized atmosphere and an effective finite mixing reservoir, based upon global parameters and the following assumptions.

Preprints (www.preprints.org) | NOT PEER-REVIEWED | Posted: 22 December 2022 doi:10.20944/preprints202212.0413.v1

1. There is a continuous bulk outflow A_{OUT} from the atmosphere to a global carbon mixing reservoir, the flow being proportional to the known listed values of atmospheric CO_2 mixing ratio, A_{CO2} (Data Ref 1,2) The constant of proportionality is the inverse residence time τ_r , which determines the initial rate of fall of the ^{14}C bomb pulse, (Figures 2&3), and is a solution parameter.
2. Carbon is returned to the atmosphere from the reservoir via an inflow of CO_2. The amount returned, A_{IN}, is calculated by balancing the budget of outflow with the known atmospheric growth of CO_2 $\Delta(A_{CO2})$ and fossil fuel emissions input A_{FF}, as shown in Figure 1. CO_2 inflow from a reservoir in which previous atmospheric CO_2 has accumulated, hinders the fall in value of ^{14}C. Hence it predominantly determines the shape of the tail of the ^{14}C bomb pulse, the rate of fall of $\delta^{13}C$, and recent $\delta^{13}C$ levels, see Figs 3, 4, 5. The reservoir size, $R_{CO2,}$ is a solution parameter.
3. Total fossil fuel emissions inflows ($CO2_{FF}$) are derived from known listings (Data Ref 3). A portion of the inflow, as described by an Airborne Factor, A_F, is directly mixed into the atmosphere, while the remaining portion (1-A_F) is absorbed directly by the reservoir. This does not imply the absorption is instantaneous, because each cycle is annual. A_F is a solution parameter. It predominantly determines the shape of the tail of the ^{14}C bomb pulse, the rate of fall of $\delta^{13}C$, and recent $\delta^{13}C$ levels Figs 3, 4, 5.
4. Inflow of $^{14}CO_2$ from known listed atmospheric atomic weapon detonations B_{14}, (Data Ref 5) are assumed to be linearly related to the bomb yield. The conversion factor Y_b (^{14}C [in 1820 background units] per megaton) is a solution parameter. It has the main effect of scaling the bomb pulse portion of the graph after 1960, Figure 3
5. Isotopic ^{13}C and ^{14}C concentrations are calculated using Dalton's mixing laws, see Appendix B. Fractionation is considered negligible at the reservoir-atmosphere boundary, fractionation factors are implicitly set to unity. The isotopic equilibrium is identical for ^{13}C ,^{14}C and ^{12}C hence there is no Revelle exception. In accounting for isotopic concentration, it is not necessary to explicitly embed Stuiver's attenuation factor, Suess dilution or a general Revelle factor (see Radiocarbon above), because they are implicitly represented. The initial values of $\delta^{13}C$, $\Delta^{14}C$ and fossil fuel $\delta^{13}C_{FF}$ content are solution parameters. These values determine the initial level in Figs 3,4 and for $\delta^{13}C_{FF}$ determine the slopes in Figs 4, & 5. b)

To be clear, the CFR does not use ad-hoc corrections to an exponential decay shape. Rather, it calculates year by year the amount of CO_2 in the biospheric reservoir, the change of ^{14}C and ^{13}C in atmosphere and reservoir and its release back to the atmosphere. The return flux is determined by "balancing the books" since atmospheric CO_2 mixing ratio is a data input. See Appendix C for annual iteration relations. The final solution is found by minimising the standard deviation between the observed and predicted values of $\delta^{13}C$, $\Delta^{14}C$ as each parameter is adjusted. The entire model is re-calculated for each of these iterations. In practice the standard deviation between observed and predicted was calculated for each graph σ_1, σ_2, and a product was taken. The square root of this product gives the total standard deviation, sd. Hence

$$\sigma_j = \sqrt{1/n \, \Sigma \, (obs_i - calc_i)^2}$$
$$sd = (\sigma_1 \times \sigma_2)^{1/2}$$

The minimisation of standard deviation was carried out using the solver function in Microsoft Excel. Only one true constant was used, atmospheric capacity, which was taken to have a value of 2.124 ppm GTC^{-1} (Ballantyne 2012). In total 340 observed data points were used and fitted returning an excellent quality of fit.

Preprints (www.preprints.org) | NOT PEER-REVIEWED | Posted: 22 December 2022 doi:10.20944/preprints202212.0413.v1

Results

The input data was prepared and selected from Data References 1-5. The model was run from 1750 to 2020, with results from 1820 to 2020 being shown; $\Delta^{14}C$ in Figs 2,3 and δ13C in Figure 4. The resulting standard deviation σ in mills is indicated in the graph captions. The graphs show excellent agreement between the CFR model and the observed global measurements. Figure 2 shows $\Delta^{14}C$ from 1820 to 2020 before, during and after the atomic bomb pulse, with 130 observed data points before 1950 and 70 observed data points from 1968 onwards(Hua 2021) The standard deviation over the entire period (which incorporates a gap from 1950 to 1968 during the bomb period) was 3.03 ‰.

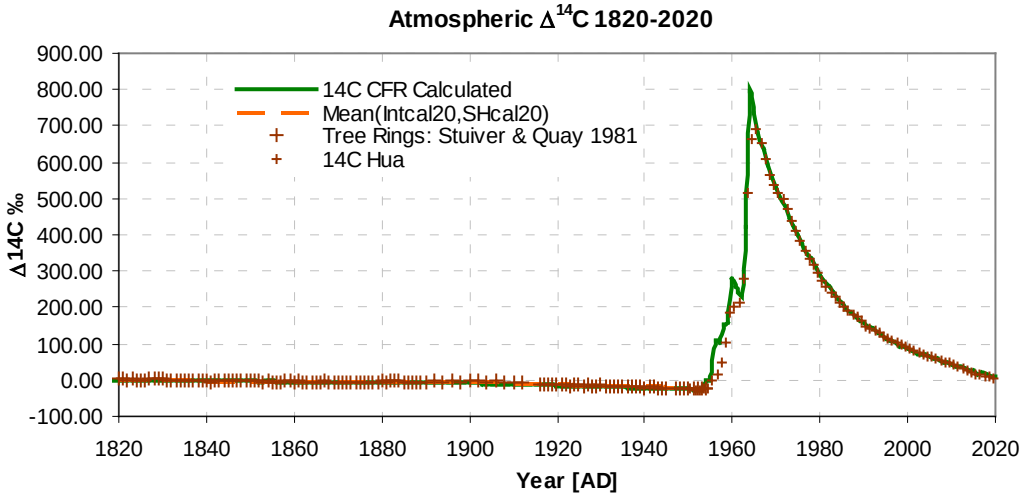

Figure 2. Atmospheric $\Delta^{14}C$ 1820-2020. CFR calculated: (solid line). Mean (Intcal20,SHCal20) (dashed line) $\sigma_{1820\text{-}1950,\ 1968\text{-}2020}$ = 3.03‰ Tree-rings: Stuiver and Quay 1981 NH (Crosses).

There is no loss of accuracy during the latter parts of the pulse tail. If the model is deliberately run with a different relative reservoir size the latter tail portion of the pulse tail ceases to fit, indicating the back flow is having the anticipated effect. Figure 3 shows just the period since the bomb pulse. Figure 4 shows the value of $\delta^{13}C$ from 1820 to 2020 with the predicted values (green line) being from the model (after the global curve fitting process) and the experimental values (brown squares and brown cross) being from NOAA PALEO and MAUNA LOA respectively showing good agreement. Figure 5 shows two key quantities from the CFR model, the anthropogenic fossil-fuel level (black line) and the level attributable to the rest (red line) termed here "natural". The values, see left and right axis labels, represent the level while the slope of the curves indicate flux rate. The superimposed data points were derived as follows. Each observed point on Figure 4 was transformed back into two separate values, one for fossil fuel content, and one for natural content using an ingenious method proposed by Tom Quirk (Quirk 2021). Essentially the method uses Equation B6 in Appendix 1 to answer the question "assuming only two source gases are involved, what quantities of the two gases (i.e. pre-industrial $\delta^{13}C_B$ and fossil fuel $\delta^{13}C_F$), would mix to form the observed $\delta^{13}C$ value?" Since Figure 4 shows a high level of agreement this is also the case in Figure 5. The similarity of the slopes of the natural level and fossil level curves shown in Figure 5, indicates similar fluxes from natural and fossil fuel inflow rates. The solution i.e. parameter values, is listed in Table 1, along with error SD and notes.

Preprints (www.preprints.org) | NOT PEER-REVIEWED | Posted: 22 December 2022 doi:10.20944/preprints202212.0413.v1

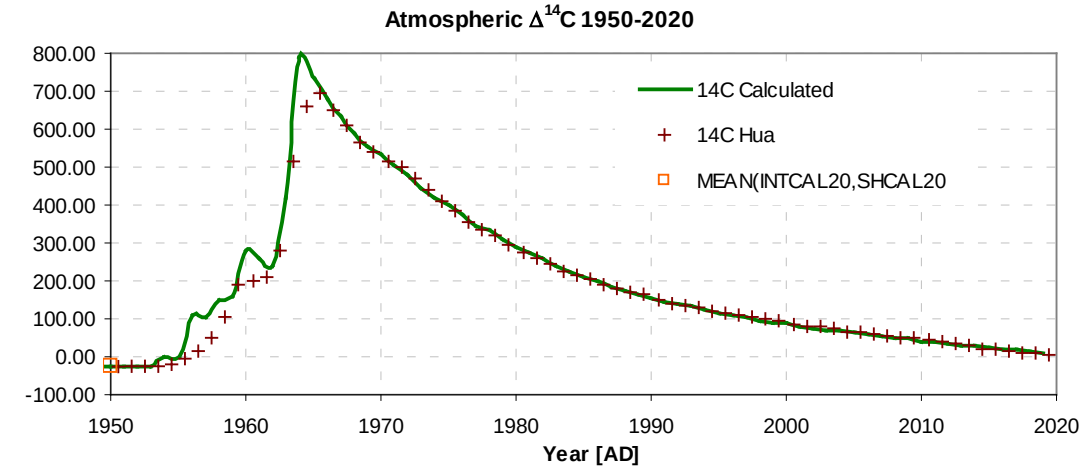

Figure 3. Atmospheric $\Delta^{14}C$. CFR calculated values: (solid line). Collated: Hua 2021 (crosses), Mean SHCAL20 and INTCAL20 (Square)

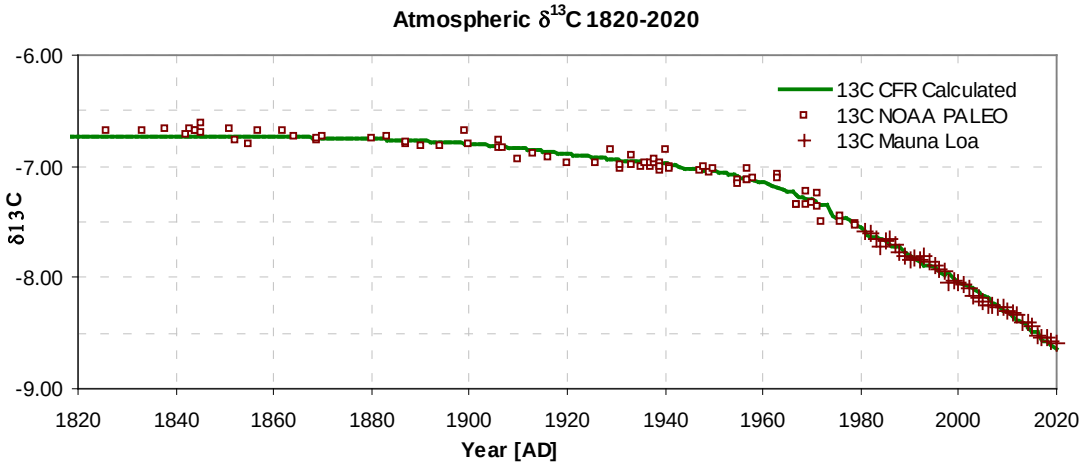

Figure 4. Atmospheric $\delta^{13}C$ 1820-2020. CFR calculated values (solid-line), Observed values: NOAA Paleo (squares), Mauna Loa (crosses) $\sigma_{1820\text{-}2020}$,= 0.05‰.

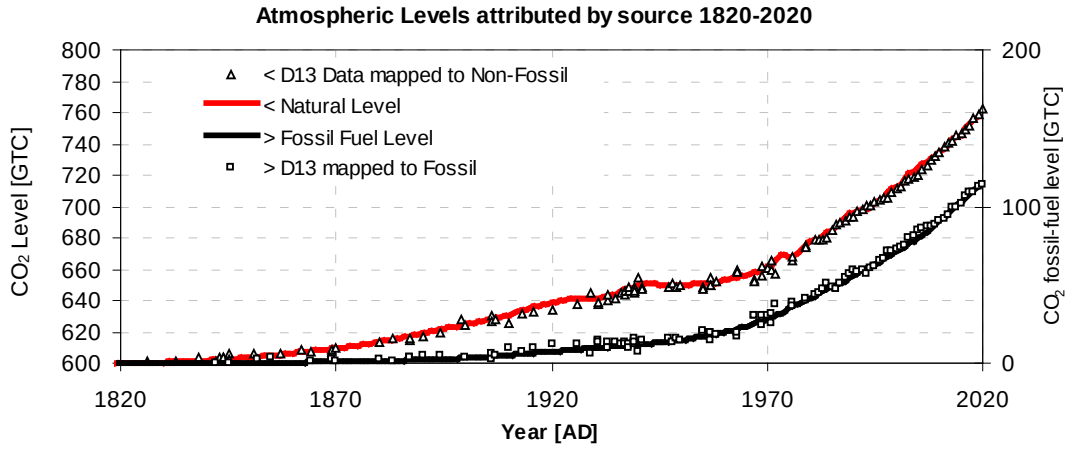

Figure 5. Atmospheric Levels derived from δ^{13}. CFR calculated (fossil black-line, non-fossil red-line). Measured values mapped via Eq. A6 using $\delta^{13}C_F$, $\delta^{13}C_B$ to fossil (square) and non-fossil (triangle). Net flow is represented by the slope indicating a similar nett flows of fossil and natural components.

 doi:10.20944/preprints202212.0413.v1

Preprints (www.preprints.org) | NOT PEER-REVIEWED | Posted: 22 December 2022 doi:10.20944/preprints202212.0413.v1

Table 1 Static Parameter Values Optimised in Solution Process

Parameter	Symbol	Value	SD +/-	Notes
Atmospheric Time constant	τ_a	14.85 yrs	2yrs	Good. Revelle & Suess 1957 ~ 10yrs, Arnold & Anderson 1957 10 - 20yrs.
Fossil-fuel Inflow Fraction	AF	0.53	0.13	Good. See Ciais 2013. P495 Airborne Fraction = 0.44.
Nuclear Bomb Yield*	Y_b	1.6	0.2	Units are relative to background 14C level
Rel. Reserve Size	R_{CO2}	6.14	1.9	$tc=\tau_a$ x R_{CO2} = 92 years. See text
^{14}C Pre-industrial	$\Delta^{14}C$	-3.1‰	7‰	Good. See INTCAL20.
^{13}C Pre-industrial	$\delta^{13}C$	-6.7‰	0.3‰	Good. See Rubino et al. 2013 Pre Ind $\delta^{13}C$ = - 6.5
^{13}C fossil fuel	$\delta^{13}C$	-20.8‰	4‰	Slightly low. See Stuiver & Polach 1977 have coal $\delta^{13}C$ = -23.

The SD value was derived by variation of the parameter, whilst holding the other values constant, until the standard deviation doubled. The resulting derived values of 5 of the parameters are in good agreement with those deduced from earlier works as referenced; this is extremely unlikely to be by chance. For the parameters Nuclear Bomb Yield, Y_b and Effective reservoir size R_{CO2} referenced values were not found.

Table 2, and Figure 6 indicate cumulative CO_2 Flows and Storage as calculated by the CFR over various periods, where non-Foss means "not due to anthropogenic fossil fuel CO_2 emissions". Cumulative fossil-fuel airborne fraction of atmospheric CO_2 has remained fairly constant irrespective of the period, with 23% to 24% remaining in the atmosphere, while 76% to 77% has been absorbed in the reservoir. However, the atmospheric increase due to fossil fuels from the past 270 years is 38%, increasing to 48% from the past 11 years. During the post-industrial period from 1750 to 2020, 52 ppm of the total CO_2 atmospheric concentration is due to fossil fuels, which corresponds to 14% of the total atmospheric CO_2 at 2020 level.

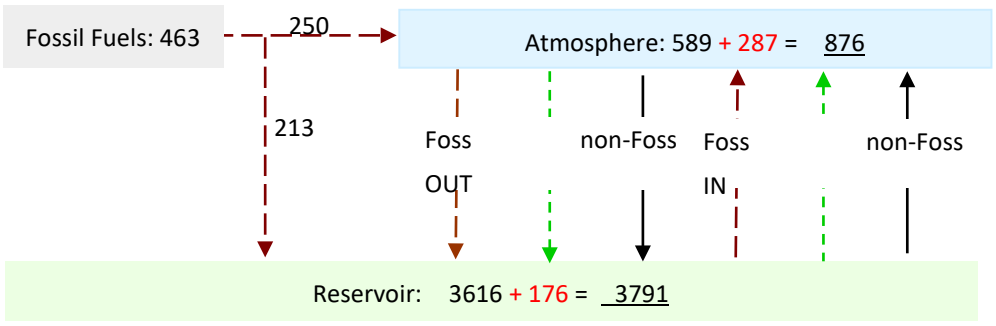

Figure 6 . Atmospheric CO_2 cumulative flux 1750 to 2020. (GTC yr^{-1}) The figures in red represent the increase over the time period, underscore indicates 2020 values. The atmospheric flux out contains more CO2ff than the flux in because the atmospheric concentration of CO2ff is higher

Preprints (www.preprints.org) | NOT PEER-REVIEWED | Posted: 22 December 2022 doi:10.20944/preprints202212.0413.v1

than the reservoir concentration, removing CO2ff from the atmosphere. Atmospheric CO2ff = 250 - 298 + 170 = 122 which corresponds to 122/876 = 13.9% of the atmosphere.

Table 2: Cumulative CO_2 Flows and Storage over various periods.

			1750-2020	1900-2020	2010-2020	
	Duration (inclusive)					
	Number of Years		269	120	10	
1	Fossil-fuel CO_2 Total		463	451	106	GTC
2	Fossil-fuel CO_2 Outflow to Reservoir		346	338	81	GTC
3	Atmos. CO_2 Increase due to Fossil Fuels	(1-2)	117	114	25	GTC
4	Atmos. CO_2 Increase due to non-Foss		171	134	25	GTC
5	Atmos. CO_2 Increase during period	(3+4)	287	248	50	GTC
6	Rel. Atmos. CO_2 Increase due to Fossil-fuels	(3/5)	41	46	50	%
7	Rel. Atmos. CO_2 Increase due to non-Foss	(4/5)	59	54	50	%
8	Rel. Fossil-fuel CO_2 being Stored	(2/1)	75	75	76	%
9	Rel. Fossil-fuel CO_2 in Atmos	(3/1)	25	25	24	%
10	Increase rel to final total atmos. CO_2*	(3)/C_{atmos}	14	13	3	%
11	Average Flow from Reservoir		43.73	47.46	57.10	GTC/yr
12	Average Flow to Reservoir		43.59	47.41	57.23	GTC/yr

* The CO_2 atmospheric mixing ratio in 2020, C_A = 412.44 ppm.

These figures take into account the backflow of fossil fuel CO_2 from reservoir to atmosphere

Discussion

The CFR method indicates the existence of an effective carbon reservoir approximately six times the atmospheric carbon content. This size is determined from curve fitting of $\Delta^{14}C$ and $\delta^{13}C$ values (Figure 2 & 4) whose rate of fall is a balance between Suess dilution and CO_2 inflow from the mixing reservoir. This effective reservoir represents those atmosphere connected physical reservoirs where isotopic mixing can occur. But which physical reservoir (s)are those? Some cyclical fluxes, such as those associated with photosynthesis on land provide little opportunity for isotopic mixing as compared to those associated with ocean absorption and emission. In a mature stable biological system, carbon cycles daily and annually between the atmosphere and biomass, and back again, and its annual input balances its annual output. Carbon isotopes "caught in the cycle" mix in the atmosphere but they may never enter a "non-atmospheric mixing reservoir". Consequently the flux values in Table 2 are smaller than those gross values in WG1AR5 Ciais 2013. Similarly, attempts to calculate the CO_2 residence time, from atmosphere size divided by gross flux (Harde 2017) or by more sophisticated methods employing eigenvectors, indicate an impulse response considerably shorter than the decay time of the bomb pulse. We suggest here this discrepancy is not because equilibration of the ^{14}C isotope

Preprints (www.preprints.org) | NOT PEER-REVIEWED | Posted: 22 December 2022 doi:10.20944/preprints202212.0413.v1

cheats the Revelle factor. Again it is because a portion of the gross flows in WG1AR5 IPCC Fig 6.1 represent cyclical quantities which offer little opportunity for isotopic mixing. The significant contributors to the "effective reservoir" are thus probably a) within the soil having 1500-2400 GTC, and b) within the ocean with 38,000 GTC (around 50 times that of the atmosphere at 589 to 830GTC). However the surface mixing layer within the ocean, estimated at 900GTC, connects very weakly with the deep ocean (Ciais 2013). The sum of the soil and surface ocean mixing layer forms a combined reservoir of around 5 times the atmosphere, as compared to the CFR model estimates of 6.14, suggesting these reservoirs may correspond to the CFR's "effective mixing reservoir". Although the CFR accounts only for fluxes from effective mixing reservoirs, it does calculate a figure for the accumulation of carbon in the effective reservoir. Using the logic above, the accumulation of carbon is probably less in those cyclical flows where there is little opportunity for isotopic mixing. This means that one can make comparisons of carbon inventory and accumulation found by CFR with figures from other authors for the ocean (see Table 3).

Table 3: Comparison of Carbon Accumulation (various Sources)

a) Carbon Inventory Increase: (GTC)					
Period					1994-2007
Ocean Carbon Inventory Increase: Watson 2020					33.7
Oceanic sink for anthropogenic carbon dioxide (Gruber 2019) +/-4					34.0
Total mixing reservoir: carbon increase: CFR - this paper					37.2
b) Cumulative CO2 Sink: (GTC)					
Period	1750-2019	1850-2014	1959-2019	1850-2019	1850-2020
Ocean GCB (+/-20)	170*	145*	105*	160*	165*
Total CFR	171.2	162.5	172	185.1	176

*Global Carbon Budget GCB (Friedlingstein P. et al, 2020), * *IPCCWGAR5(Ciais 2013), # (Watson et al. 2020)

In Table 3 a) the total increase in ocean carbon inventory from CFR is compared with recently revised estimates (Gruber et al 2019, Watson et al. 2020). The CFR value is some 10% larger than these values. However the CFR model reservoir size represents both land and ocean mixing reservoirs. In b) values from the Global Carbon Budget (GCB) over the longer term period of 270 years show agreement with CFR to within 0.8 %. However over shorter time periods e.g. from 1959 to 2019 CHR figures are some 35% higher, again perhaps because the CFR reservoir may include land based accumulation (e.g. soil). In GCB, Land-Use-Change (LUC) balances Terrestrial Sink to within 10% and are listed separately, while Fossil Fuel Emissions E_{FOS} are divided between the growth in atmosphere G_{ATM} and Ocean Sink $_{SOCEAN}$. Between 1750 and 2019, GCB has atmospheric growth, G_{ATM} as 64% of E_{FOS} while in CFR it forms 62% of E_{FOS}.

Conclusion

This paper shows that the global CO_2 flux, despite its apparent complexity, can be approximated using a top-down approach by a global atmospheric CO_2 flux flowing between an idealized atmosphere and an idealized finite reservoir store, employing a classic rate ordinary differential equation. The model uses a mechanism of curve fitting to derive seven parameters which provides a high degree of agreement with values of ^{14}C and ^{13}C over periods of 200 years. The CFR model accounts for the observed variation of $\Delta^{14}C$ and $\delta^{13}C$ with time by using a CO_2 influx from an effective reservoir, which having higher values than those for fossil fuel (having been previously a nett absorber) hinder the fall of the $\Delta^{14}C$ and $\delta^{13}C$ curves. The CFR model not only shows that an incoming CO_2 flux is a plausible explanation, it

 doi:10.20944/preprints202212.0413.v1

accurately calculates the influx. It has been asserted that approaches using analysis of the ^{14}C bomb pulse are not valid due to the different behaviour of ^{14}C and ^{12}C. The results show that this challenge is unfounded, and the paper identifies theoretical mistakes which led to this assertion, restoring the conviction that such anomalous behaviour of an isotope is unlikely. The effects of this mis-step upon climate science may be considerable and wide reaching, since the isotopic ratiometric exception has almost certainly entered the internal coding for various climate models. Such models have been widely used for flux calibration using the partition method (Zeng et al, 2020) and for scenario testing of fossil fuel emissions. Although the CFR model is not itself a climate model it can usefully provide indications of effective bulk global parameters and provides a focus on the physics of internal processes. The CFR method thus offers a means by which estimates of effective bulk global quantities can be compared. The model can be downloaded as a Microsoft Excel Spreadsheet from https://www.geomatix.net/atmos2boxmodel.htm.

Acknowledgments

I would like to thank my colleagues Dr. Andrew Layfield (Engineering and Environmental Studies), City University, Hong Kong, and Dr. Michael Oates (Geologist) of Barrow-upon-Humber, UK for their detailed comments and proof reading. The author would like to thank and acknowledge all the data providers indicated in "Data References", without whom this work could never have been carried out. This research was self-funded and received no external funding. The author declares no conflict of interest. The author would like to thank the publisher for waiving the APC which was funded by the publisher.

APPENDIX

Appendix A. Notes on Tans 2022 and Tans 1993

In 1993 Tans derived an expression for $C_A\, dR_A/dt$ (where C_A is the atmospheric CO_2 content and R_A is the isotopic composition of atmospheric gaseous CO_2 eq.13). Tans 2022 eq. 1 is simplified by setting all terms with subscripts lb or ph to zero. In either case Tans derives

$$C_a dR_a/dt = F_{fos}\,(R_{fos} - R_a) - (F_{ao} - F_{oa})\,R_a\,(\alpha_{ao} - 1) + F_{oa}\,\alpha_{ao}\,(R_a^{eq} - R_a)) \qquad (T1)$$

It is claimed the last term, because it is a difference of ratiometrics, multiplied by a one way flux provides evidence of "*pure isotopic equilibration that always takes place regardless of what the net total flux is*". in 2022 he states *"The Revelle factor does not apply to isotopic equilibration because a 12CO2 molecule is replaced by a 13CO2 or vice versa. As a result, an isotopic anomaly disappears from the atmosphere more quickly than a total CO2 anomaly."* In the derivation Tans has

$$d^{13}C_a/dt = d\,(R_aC_a)/dt = C_a dR_a/dt + R_a dC_a/dt \qquad (A2)$$

$$d^{13}C_a/dt = R_{fos}F_{fos} + \alpha_{oa}R_oF_{oa} - \alpha_{ao}R_aF_{ao} \qquad (A3)$$

Preprints (www.preprints.org) | NOT PEER-REVIEWED | Posted: 22 December 2022 doi:10.20944/preprints202212.0413.v1

$dC_a/dt = F_{fos} + F_{oa} - F_{ao}$ (A4)

At equilibrium between the two reservoirs R_{fos}=0, $d^{13}C_a/dt$ =0 and dC_a/dt =0 so we have

$\alpha_{oa}R_o^{eq}F_{oa}^{eq} = \alpha_{ao}R_a^{eq}F_{ao}^{eq}$ (A5)

$F_{oa}^{eq} = F_{ao}^{eq}$ (A6)

Giving

$\alpha_{oa}R_o^{eq} = \alpha_{ao}R_a^{eq}$ (A7)

However Tans has written eq A7 as

$R_a^{eq} = (\alpha_{oa}/\alpha_{ao})R_o$ [R_o^{eq} is replaced by R_o]

The effect of the incorrect substitution is to enable the grouping in the last term (T1). Its effect upon the rate of isotopic transfer $d^{13}C_a/dt$ can be evaluated by adding Tans' expression for $C_a dR_a/dt$ (eq. T1) to the value of $R_a dC_a/dt$ (eq. A4 multiplied by R_a) to provide a new "test" value for $d^{13}C_a/dt$

$$"d^{13}C_a/dt" = F_{fos}(R_{fos} - R_a) - (F_{ao} - F_{oa})R_a(\alpha_{ao} - 1) + F_{oa}\alpha_{ao}(R_a^{eq} - R_a) + R_a(F_{fos} + F_{oa} - F_{ao})$$

After some re-arranging and using the correct substitution of (A7) gives

$$"d^{13}C_a/dt" = F_{fos}R_{fos} + \alpha_{oa}R_o^{eq}F_{oa} - \alpha_{ao}R_aF_{ao}$$

It can be seen that the term R_o in (A3) is replaced by its equilibrium value R_o^{eq} . This is not justifiable as it prevents the ocean from exhibiting any isotopic variation when coming to an equilibrium, effectively clamping its isotopic ratio to the value R_o^{eq}, implying its volume is infinite. Furthermore Tans' expression for $C_a dR_a/dt$ (eq.A1) does not fully represent $d^{13}C_a/dt$ (which is the quantity required) because $R_a dC_a/dt$ is missing from the calculation. The same arguments apply to ^{14}C as ^{13}C. Equations A3 and A4 are the correct versions and are used throughout this paper neglecting fractionation (with $\alpha_{oa}=\alpha_{ao}$= 1) and in the production of the presented results.

Appendix B. Notes on Isotopic Mixtures and Radiocarbon Levels

Dalton's "Law of Partial Pressures" indicates that, when two gases having partial pressure P_A and P_B and concentration R_A and R_B, are mixed, then the total pressure, P_T of the mixture will be given by

$P_T = P_A + P_B$

and its concentration R_M of the mixture or model is

$R_M = (R_A P_A + R_B P_B) / P_T$

Preprints (www.preprints.org) | NOT PEER-REVIEWED | Posted: 22 December 2022 doi:10.20944/preprints202212.0413.v1

Note: If the isotopic amount is described by an offset scale e.g. R = (m.δa + c) the above becomes

$(m\ \delta m + c)\ P_T = (\ m\ \delta a + c)\ P_A + (\ m\ \delta a + c)\ P_B$

which after rearranging gives equations of similar form, i.e.

$\delta_m\ Pt = \delta a\ P_A + \delta b\ P_B$ (B1)

$\delta_m = (\delta a\ P_A + \delta b\ P_B) / P_T$ (B2)

Conversely, for a mixture of total pressure P_T, whose concentration is δm, given the concentration of its two constituents δa and δb, the pressure of the constituent P_A, is given by (Quirk T. 2021)

$P_A = P_T\ (\ \delta m - \delta a\ ) / (\ \delta a - \delta b\ )$ (B3)

Conventionally $\delta^{14}C$ is defined as an offset scale whose value is zero when A_s, the specific activity of the atmosphere or reservoir is equal to A_{abs}, the absolute specific standard, with both being in units of Bq per unit mass of carbon. Hence we may write

$A = \delta^{14}C + 1 = \quad (A_s/A_{abs})$

where A refers to the relative specific ^{14}C activity. Thus A contains no allowance for radioactive decay or fractionation. For the mixture M obtained by mixing natural N and fossil fuel derived F components we may write using Equation A2 for A_M and $\delta^{13}C_M$

$A_M \quad = (A_N\ P_N / P_T) - 1$ (B4)

$\delta^{13}C_M = \quad (\delta^{13}C_F\ P_F + \delta^{13}C_N\ P_N) / P_T$ (B5)

bearing in mind that $A_F = 0$. The inverse for $\delta^{13}C_M$,, used in Figure 6 to map from observed atmospheric values of δ^{13} to CO_2 levels by source from Equation A(3) is

$P_N = P_T\ (\ \delta^{13}C_M - \delta^{13}C_F\ ) / (\ \delta^{13}C_N - \delta^{13}C_F\ )$ (B6)

Fractionation

It is desired to compare values of A_M with collated measured values of $\Delta^{14}C$. However $\Delta^{14}C$ incorporates a fractionation correction to "translate the measured activity to the activity the sample would have had if it had been wood" (Lund 2011) and is a function of $\delta^{13}C$. Therefore a fractionation correction must be applied to A_M, where δ^{13} for wood is taken as -25‰, given by

$\Delta^{14}C_M = A_M\ .\ \{\ (1+\ \delta^{13}C_W)/(1+\ \delta^{13}C_M)\ \}^2 \quad - 1$

Preprints (www.preprints.org) | NOT PEER-REVIEWED | Posted: 22 December 2022 doi:10.20944/preprints202212.0413.v1

This formula decreases the values by around 35‰ compared to the values for A_M.

Age Correction

Sample age correction, common in radiocarbon calculations, is not included in the CFR or the definition of $\Delta^{14}C$. The ^{14}C half-life of 5700+/-30 years (Kutschera, W., 2013) translates to a decay of around 2% over the period 1820 to 2020. However, the steady level of stratospheric ^{14}C production roughly balances the amount of ^{14}C decay since the two are in approximate equilibrium, providing a buffering effect. Disregarding ^{14}C decay introduces an error at most in the low percentage region and probably considerably smaller and is regarded as negligible. Therefore neither ^{14}C decay nor natural stratospheric ^{14}C production were included in the CFR model. Values of A were not artificially corrected for ^{14}C decay before comparison with $\Delta^{14}C$.

Appendix C: Implementation

The implementation process involves a number of calculations at each iteration which are based upon "Daltons Law of Partial Pressures". The amount of CO_2 in the atmosphere is A_{CO2} and that in the reservoir is R_{CO2}, with respective increases being written as $\Delta(A_{CO2})$ and $\Delta(R_{CO2})$ at each iteration, i, then the iteration relationships are:-

$\Delta(R_{CO2}) = R_{CO2}[i] - R_{CO2}[i-1]$ $\Delta(A_{CO2}) = A_{CO2}[i] - A_{CO2}[i-1]$

$A_{OUT}[i] = A_{CO2}[i] / tc$ $A_{IN}[i] = A_{OUT}[i] + A_{CO2}[i] - A_{CO2}[i-1] - A_F\, CO2_{FF}[i]$

$R_{CO2}[i] = R_{CO2}[i-1] + A_{OUT}[i] - A_{IN}[i] + (1-A_F)CO2_{FF}[i]$

For the ratio of ^{14}C to ^{12}C in Atmosphere $A_{14}[i]$ and Reservoir $R_{14}[i]$ we have:-

$A_{14}[i] = (A_{14}[i-1].A_{CO2}[i-1] + A_{IN}[i-1].R_{14}[i-1] - A_{OUT}[i-1].A_{14}[i-1] + B_{14}[i-1]) / A_{CO2}[i]$

(^{14}C previously + ^{14}C coming in - ^{14}C going out + Bomb ^{14}C) / Atmos C

$R_{14}[i] = (R_{14}[i-1].R_{CO2}[i-1] - A_{IN}[i-1].R_{14}[i-1] + A_{OUT}[i-1].A_{14}[i-1]) / R_{CO2}[i]$

(^{14}C previously + ^{14}C coming in - ^{14}C going out) /Reservoir C

Similarly the relative atmospheric and reservoir fossil fuel content $A_{FF}[i]$, $R_{FF}[i]$, on a scale of 0 to 1, are given by:-

$A_{FF}[i] = (A_{FF}[i-1].A_{CO2}[i-1] + A_{IN}[i-1].R_{FF}[i-1] - A_{OUT}[i-1].A_{FF}[i-1] + A_F\, CO2_{FF}[i]) / A_{CO2}[i]$

$R_{FF}[i] = (R_{FF}[i-1].R_{CO2}[i-1] - A_{IN}[i-1].R_{FF}[i-1] + A_{OUT}[i-1].A_{FF}[i-1] + (1-A_F)\, CO2_{FF}[i]) / R_{CO2}[i]$

$FL[i] = A_{CO2}[i]\ A_{FF}[i]$ $NL[i] = A_{CO2}[i]\ (1- A_{FF}[i])$

where the absolute fossil fuel level, FL[i], and natural non-fossil level, NL[i], are shown in the final equation. The isotopic ratiometric measures for ^{13}C $\delta^{13}C$, and ^{14}C $\Delta^{14}C$ are given by:-

$\delta^{13}C = \delta^{13}C_{FF} . A_{FF} + \delta^{13}C_N\ (1- A_{FF})$ $\Delta^{14}C = (A_{14} -1)$

Initial Conditions: $A_{IN}[0] = A_{OUT}[0]$, $A_{14}[0] = 1$, $R_{14}[0] = 1$, $A_{FF}[0] = 0$, $R_{FF}[0] = 0$

Preprints (www.preprints.org) | NOT PEER-REVIEWED | Posted: 22 December 2022 doi:10.20944/preprints202212.0413.v1

where A_{OUT} is the atmospheric outflow, A_{CO2} is the atmospheric CO_2 mixing ratio, A_{IN} is the atmospheric inflow, R_{CO2} is the reservoir CO_2 mixing ratio, R_{FF} is the relative fossil fuel level in the reservoir, R_{14} is the $f^{14}C$ level in the reservoir, F_{RSVR} is the Fossil fuel CO_2 mixing ratio in the reservoir, A_{14} is the $f^{14}C$ level in the atmosphere, B_{14} is the annual ^{14}C production due to atomic weapons testing $\Delta^{14}C$ is the $^{14}C/^{12}C$ ratio and $\delta^{13}C$ = is the $^{13}C/^{12}C$ ratio and the square brackets "[ ]" refer to the value at each iteration. The constant α is an output which in the case of an infinite reservoir represents the time constant in equations C1, C2.

Appendix D: Attenuation Factor of 14C and 13C

Stuiver & Quay proposed an "attenuation factor" for Δ14C because the Suess dilution of atmospheric CO_2 was not as great as expected. (Stuiver & Quay 198). Between 1820 and 1950 the actual reduction in Δ14C was around 20‰ using IPCCC-WG1AR5 WG1AR5 Figs. 4&6b, pp 493-4 (Ciais 2013) or Intcal20 data. During this time the atmospheric level increased from 600 to 667 GTC while listed CO2ff emissions totalled 61GTC. Setting in Equation B5 $\delta^{14}C_F$ = -1000, P_F = 6, $\delta^{14}C_N$= 0 , P_N= 600, P_T=667 gives a reduction in Δ14C of 89‰, much larger than the measured decrease of 20‰. A similar argument can be made for $\delta^{13}C$. The actual annual reduction can be measured from Figure 4 or from IPCCC-WG1AR5 Figure 6b and is around 0.025‰ per year. Both the IPCC curve and Figure 4 from this paper indicate that the annual CO_2 emissions from fossil fuels in 2000AD was approximately 6 GTC yr^{-1} around one 125th of the atmospheric size of around 750 GTC which was increasing at around 3GTC per year. For fossils d13 = -26V (or higher) while for the atmosphere in 2000AD δ^{13} = -8 (see) Setting in Equation B5 $\delta^{13}C_F$ = -26, P_F = 6, $\delta^{13}C_N$=-8, P_N= 750, P_T=756 gives $\delta^{13}C_M$ = -8.14‰, indicating a decrease of 0.14‰ per year which is considerably greater than 0.025‰ per year. Some have suggested fossil fuels have even lower δ^{13} figures of approaching -44‰ (Bush et al 2007) which would make this discrepancy greater. Even allowing for the airborne fraction (i.e. the fact that the atmospheric increase was attributed to only half of the CO2ff) there still is a considerable discrepancy in both cases. The analysis given above of $\delta^{13}C$ and Δ14C is entirely independent of the CFR model itself and is simply based on published data. It is postulated here that the above discrepancy can be accounted for by a CO_2 inflow from a reservoir in which previous atmospheric CO2 has accumulated, which having higher Δ14C and $\delta^{13}C$ values than those for fossil fuel would hinder the fall. The CFR model not only shows that this inflow is a plausible explanation, it accurately calculates the inflow, the $\delta^{13}C$ and the value of Δ14C.

References

Archer, D et al. 2009. Atmospheric lifetime of fossil fuel carbon dioxide. Annu. Rev. Earth Planet. Sci., 2009. 37:117–134.

Arnold J.R. & Anderson E.C. 1957. The Distribution of Carbon-14 in Nature. **Tellus IX 1957.**

Ballantyne, A. P et al. 2012. Increase in observed net carbon dioxide uptake by land and oceans during the last 50 years. Nature, 488, 70–72.

Bauska et al. 2014 Carbon isotopes characterize rapid changes in atmospheric carbon dioxide during the last deglaciation. PNAS | March 29, 2016 | vol. 113 | no. 13 | 3465–3470

Bengston et al. 2020 Lower oceanic δ13C during the last interglacial period compared to the Holocene. Clim. Past, 17, 507–528, https://doi.org/10.5194/cp-17-507-2021, 2021.

Bolin B, Eriksson E. 1959. Changes in the carbon dioxide content of the atmosphere and sea due to fossil fuel combustion. In Rossby Memorial Volume, ed. B Bolin:130-42. New York: Rockefeller Institute Press, Oxford University Press. Number of 130-42 pp.

Bush S.E. et al 2007. Sources of variation in d13C of fossil fuel emissions in Salt Lake City, USA , Applied Geochemistry 22 (2007) 715–723

Ciais, P. et al, 2013. Carbon and Other Biogeochemical Cycles. Chapter 6. Climate Change 2013: The Physical Science Basis. [Stocker et. al] WG1 AR5 IPCC 2013.

Friedlingstein P. et al, 2020. Global Carbon Budget 2020, Earth Syst. Sci. Data, 12, 3269–3340, https://doi.org/10.5194/essd-12-3269-2020, 2020

Gruber, N. et al. 2019. The oceanic sink for anthropogenic CO2 from 1994 to 2007. Science 363, 1193–1199 (2019).

Harde H. 2017. Scrutinizing the carbon cycle and CO2 residence-time in the atmosphere , Global and Planetary Change 152 (2017) 19–26

Harvey Danny LD 2000, Global Warming: The Hard Science, Pearson Education Limited, UK. ISBN 0582-38167-3

Hua Q. et al. Atmospheric Radiocarbon For The Period 1950–2019, Radiocarbon Vol 0 Nr00 2021. Submitted. Private Communication

Joos F. 1994. , Imbalance in the Budget, Nature Vol 370 21July 1994

Kutschera, W., (2013) Applications of accelerator mass spectrometry. *International Journal of Mass Spectrometry* 349, 203-218.

Levin I. et al. 2010 Observations and modelling of the global distribution and long-term trend of atmospheric 14CO2. Tellus B, 62: 26-46 2010.

Marcott A S et al., 2014. Centennial-scale changes in the global carbon cycle during the last deglaciation. Nature,Vol 514,30October 2014

Quirk T. 2021 Suggested method using inversion formulae for d13C. Private Communication 2021

Rubino, M et al 2013. A revised 1000 year atmospheric δ13C-CO2 record from Law Dome and South Pole, Antarctica. Journal of Geophysical Research: Atmospheres, 118(15), pp.8482-8499. 2013

Stenström K. E. 2011. A guide to radiocarbon units and calculations, Lund University, Department of Physics, Division of Nuclear Physics. Sweden. 2011

Revelle, R & Suess H, 1957. Carbon Dioxide Exchange Between Atmosphere and Ocean and the Question of an Increase of Atmospheric CO2 during the Past Decades. Tellus IX(1957).1

Stuiver, M. & Quay, P.D. 1981. Atmospheric ^{14}C changes resulting from fossil fuel CO2 release and cosmic ray flux variability. Earth and Planetary Science Letters, 53 (1981) 349-362

Stuiver M & Polach H A. 1977 Discussion: Reporting of 14C Data, Radiocarbon, Vol19 No 3 1977 P355-363

Stuiver et al. 1998 "Intcal98 Radiocarbon Age Calibration, 24,000-0 Cal Bp", Radiocarbon, Vol. 40, No. 3, 1998, P.1041-1083

Tans, P., Berry J., Keeling R. Oceanic 13C/12C Observation: A new window on ocean CO2 uptake. Global Biogeochemical Cycles Vol 7 No2 P353-368) June 1993

Tans P. 2022. Reminiscing On The Use And Abuse Of 14c And 13c In Atmospheric Co2. Radiocarbon, Vol 64, Nr 4, 2022, p 747–760 DOI:10.1017/RDC.2022.7

Suess, H.E. 1955 Radiocarbon concentration in modern wood. Science 122, 415.

Svetlik I. 2010 Estimation of Long-Term Trends in the Tropospheric 14CO2 Activity Concentration. Proceedings of the 20th International Radiocarbon Conference, edited by A J T Jull, RADIOCARBON, Vol 52, Nr 2–3, 2010, p 815–822

Zeng J. et al. 2020. Global terrestrial carbon fluxes of 1999–2019 estimated by upscaling eddy covariance data with a random forest . Scientific Data (2020) 7:313 | https://doi.org/10.1038/s41597-020-00653-5

 doi:10.20944/preprints202212.0413.v1

Data References

1. Institute for Atmospheric and Climate Science (IAC), CO2 Mean Global AD0 to AD2014 ftp://data.iac.ethz.ch/CMIP6/input4MIPs/UoM/GHGConc/CMIP/yr/atmos/UoM-CMIP-1-1-0/GHGConc/gr3-GMNHSH/v20160701/ mole_fraction_of_ carbon_dioxide_in_air_input 4MIPs_GHGConcentrations_CMIP_UoM-CMIP-1-1-0_gr3-GMNHSH_0000-2014.csv
2. NOOAA GML. Accessed 04-March-2022. https://gml.noaa.gov/ccgg/trends/gl_data.html File: https://gml.noaa.gov/web-data/ccgg/trends/co2/co2_annmean_gl.txt
3. Global Carbon Budget: National_Carbon_Emissions_2021v0.4.xlsx Historical Budget, Global Fossil Emissions Visited 04 March 2022.Friedlingstein et al (2021),
4. World Data Service for Paleoclimatology, Boulder and NOAA Paleoclimatology Program, National Centers for Environmental Information (NCEI) https://www1.ncdc.noaa.gov/pub/data/paleo/icecore/antarctica/law/law2018d13c-co2.txt, https://doi.org/10.25919/5bfe29ff807fb
5. UNSCEAR: United Nations Scientific Committee on the Effects of Atomic Radiation 2000 Report To The General Assembly. Volume I: Sources. Annex C: Exposures To The Public From Man-Made Sources Of Radiation 207 Sources And Effects Of Ionizing Radiation. . Table 4. Annual Fission And Fusion Yields.
6. Calib: INTCAL20/SGCAL20. Stuiver, M. et al, 2022 CALIB 8.2 [WWW program] at http://calib.org, accessed 2022-3-4 Rev 8.1.0 intcal20.14c, shcal20.14c